

Wetting Behavior of Argon on Graphite.

L. BRUSCHI(*), G. TORZO(*) and M. H. W. CHAN(**)

(*) *Dipartimento di Fisica, Università di Padova, 35131 Padova, Italy*

(**) *Department of Physics, Penn State University
University Park, PA 16802, USA*

(received 29 December 1987; accepted in final form 27 April 1988)

PACS. 68.45 – Solid-fluid interface processes.

PACS. 68.55 – Thin film growth, structure, and epitaxy.

Abstract. – A mechanically driven graphite fiber microbalance is used to investigate the wetting behavior of argon on graphite. We found evidence of complete wetting above the bulk triple point T_3 and incomplete wetting below. Below T_3 the thickness d of the saturated adsorbed film is found to obey the power law $d \propto (t)^x$, with $x = -1/3$, in the reduced temperature range $10^{-5} < t = (T_3 - T)/T_3 < 10^{-2}$. Above T_3 the film thickness diverges as $d \propto [\ln(P_0/P)]^x$, with $x = -1/3$.

There are two different growth modes of an adsorbate film on a solid surface. A film is said to wet the surface if its thickness diverges as the saturated vapor pressure is approached. If the film thickness remains finite, nonwetting growth is said to occur. A wetting transition occurs when there is a crossover from one kind of growth mode to the other.

Recent model [1] predicts, in the low-temperature limit, that it is the relative strength of adsorbate-substrate and adsorbate-adsorbate interactions that determines whether a particular physisorption system will exhibit wetting or nonwetting growth.

This simple idea is not adequate in dealing with real adsorption systems with solid adsorbed films. In most of the physisorption systems studied so far, including those where adsorbate-substrate interaction dominates, clear evidence of nonwetting growth of the film for $T < T_3$ is found, T_3 being the bulk triple-point temperature. Above T_3 , wetting growth is observed [2, 3]. The most reasonable explanation is that in spite of the strong substrate attraction, the strain induced by structural mismatch between successive layers eventually becomes too costly in free energy and wetting is suppressed [4].

In the recent reflection high-energy electron diffraction (RHEED) study [5], however, layer-by-layer growth of Ar, Kr, and Xe on graphite up to 10 layers with no evidence of clusters were observed down to 10 K, while for N_2 and Ne bulk clusters appear in coexistence with a bilayer film. These results led some authors to suggest that, while complete wetting growth at low temperature is not possible for systems of either very strong or very weak adsorbate-substrate interactions (re-entrant nonwetting), it is possible for systems of intermediate adsorbate-substrate interaction.

In this paper we report a study of the growth mode of argon on graphite near T_3 , well beyond the first 10 layers. Our result shows nonwetting growth for $T < T_3$ and a wetting transition at $T = T_3$.

The technique employed in this work is substantially that of the vibrating wire viscometer [6, 7], previously used by us to study the critical behavior of the ^4He viscosity close to the lambda transition [8], and as microbalance in CO_2 at the liquid-vapor coexistence curve [9].

The essential features of the method are described below: a thin graphite fiber is excited into vibration in a transverse magnetic field and its motion is detected by measuring the induced voltage signal. From measurements of the resonant frequency F , the thickness of the gas layer adsorbed onto the fiber can be calculated. The resonant frequency in vacuum is $F_0 = \sqrt{(\tau/4Lm)}$, where L is the length of the fiber and m is its mass. Neglecting the hydrodynamic mass, the excess mass due to the adsorbed film is, therefore, $\Delta m = m[(F_0/F)^2 - 1] \approx 2m(\Delta F/F)$.

This method was first used by Bartosh and Gregory to perform adsorption isotherms of oxygen on graphite [10], and later by Taborek and Senator to study helium film growth [11]. In the oxygen experiment, a wetting transition was found at T_3 , but the exponent characterizing power law film growth was significantly different from the expected value of $-1/3$. The reduced temperature range explored was $1.5 \cdot 10^{-3} < t = (T_3 - T)/T_3 < 1.8 \cdot 10^{-2}$, and the fiber was electrically excited.

We improved the method by adopting mechanical excitation of the fiber through a piezoelectric transducer to avoid Joule-heating and mainly the synchronous pick-up due to the resistance of the graphite fiber. Frequency locking is accomplished by using a new twin phase-locked-loop technique [12] which minimizes the residual phase error effects giving a resonant frequency resolution of 1 p.p.m. even at low Q values ($10^2 < Q < 10^5$).

Since the adsorbed mass is measured by the frequency shift $F - F_0$, a high stability of F_0 is required. In our set-up one end of the fiber is attached to a soft spring which provides a constant tension τ , thus greatly reducing the effects of temperature on F_0 . The temperature coefficient of F_0 is typically $dF_0/F_0 dT = -10^{-5} \text{ K}^{-1}$. Another important feature of our set-up is that it is less sensitive to changes of the fiber stiffness, probably due to the high working frequency, and therefore the film contribution to the frequency shift is essentially due to the mass loading.

The copper sample-cell is thermally regulated [13] to better than 1 mK, and the filling line is carefully kept slightly warmer than the cell. The temperature scale is estimated to be accurate to 30 mK. The pressure is measured by a MKS capacitive pressure gauge whose sensing heads are thermally regulated to improve long-term stability. The heads are calibrated *vs.* a mercury gauge with an accuracy of 0.1 Torr.

In the pressure range covered in our measurements the hydrodynamic frequency shift cannot be neglected when calculating the adsorbed mass. The correction can be written, following Stokes notation [14], $\Delta m = m[(F_0/F)^2 - 1] - km_v$, where m_v is the mass of gas displaced by the fiber and k is a known function of the frequency, of the fiber radius r , and of the gas density ρ_v and viscosity η_v . While ρ_v can be easily calculated from the measured pressure, η_v is not accurately known in the temperature and pressure range covered by our measurements. We, therefore, obtained k numerically from the Stokes function k' given by $k' = (m/m_v)(\delta F/F)(F_0/F)^2$, where δF is the resonance width [7].

We used mesophase pitch derived fibers (PDF) manufactured by Union Carbide (P100 and P120 types) with a nominal diameter of $10 \mu\text{m}$ and a density of 2.17 g/cm^3 . The fiber is cleaned *in situ*, by heating to high temperature (above 500°C) in vacuum with a current of a few mA. The argon gas, produced by Matheson, is Research quality, with a nominal purity of 99.9999%.

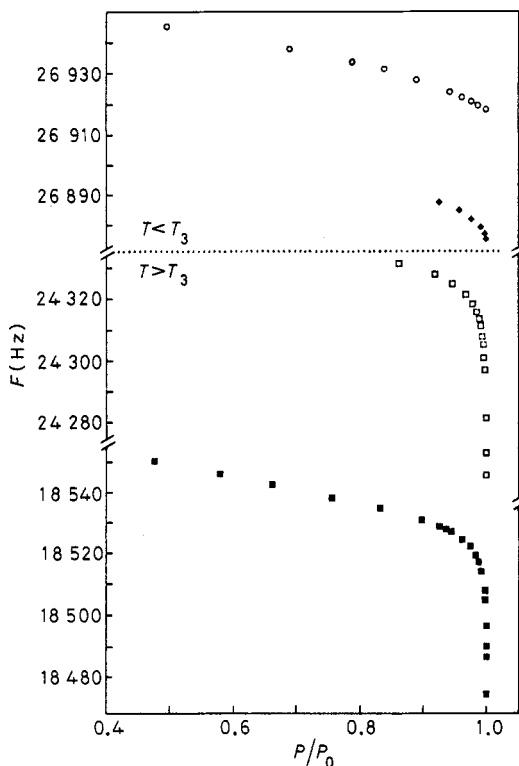


Fig. 1. – The fiber resonant frequency F vs. the reduced pressure P/P_0 measured along four isotherms above and below T_3 . $T = 77.39$ K ($P_0 = 201.1$ Torr) (\circ), $T = 83.30$ K ($P_0 = 483.5$ Torr) (\blacklozenge) and $T = 83.95$ K ($P_0 = 525.85$ Torr) (\blacksquare) with P100 fiber. $T = 83.84$ K ($P_0 = 515.7$ Torr) (\square) with P120 fiber. The relative frequency shift corresponding to one adsorbed layer is $\Delta F/F = 2 \cdot 10^{-5}$.

The results are summarized in fig. 1, where the resonant frequency F is plotted vs. the reduced vapor pressure P/P_0 for two isotherms below T_3 and two above T_3 . The data are reproducible with respect to pressure and temperature cycling. Data above and below T_3 in fig. 1 were obtained with two different P100 fibers and with one P120 fiber. Our measured P_0 values are in good agreement with published values [15], whose mean accuracy is $dP_0/P_0 \approx 0.5\%$.

The maximum thickness of the adsorbed layer, proportional to the frequency shift at P_0 , increases continuously when approaching T_3 from below. This is shown in fig. 2 where the values $F(P_0)$ are plotted vs. the reduced temperature T/T_3 .

These measurements are rather delicate and time-consuming because the system requires many hours to reach complete thermodynamic equilibrium close to P_0 [16]. When the system is at $P = P_0$, every small quantity of gas introduced into the cell produces a temporary increase of pressure and a large drop of frequency: during the transient the pressure falls slowly down to the equilibrium value, while the frequency grows back to the original value. However, the reproducibility of the frequency measured at equilibrium has been tested both adding and subtracting gas. Therefore, only some of the data reported in fig. 2 have been taken from adsorption isotherms, and most have been obtained by following the solid-vapor coexistence curve.

Above T_3 , in the wetting growth region, the adsorbed film thickness should diverge as $d = (K_B T / \alpha \log(P_0/P))^x$, where α characterizes the strength of the adsorbate-substrate interaction and x should have the value $-1/3$ for van der Waals interaction.

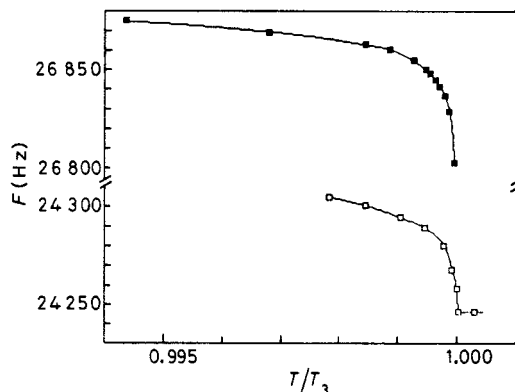


Fig. 2. – The resonant frequency measured, with P100 (■) and P120 (□) fibers, at the maximum film thickness as a function of the reduced temperature T/T_3 . The relative frequency shift corresponding to one adsorbed layer is $\Delta F/F = 2 \cdot 10^{-5}$.

Since it is necessary to include the effect of surface tension and gravity, resulting from the curved film-vapor interface, and the fact that the fiber is not at the bottom of the cell, the correct dependence [17] for d is

$$d = \left(\frac{K_B T}{\alpha} \right)^x \left(\log \frac{P_0}{P} + \frac{\sigma V}{r K_B T} + \frac{m_{Ar} g h}{K_B T} \right)^x = \left(\frac{K_B T}{\alpha} \log \frac{P_0^*}{P} \right)^x.$$

The divergence is, therefore, expected to occur at the «corrected saturated vapor pressure» P_0^* , slightly larger than the bulk saturated vapor pressure P_0 . Because P_0 is the maximum achievable pressure, the film thickness remains finite at saturation, in spite of complete wetting.

Taking a value of 13.4 dyn/cm for the surface tension σ , $50 (\text{\AA})^3$ for the volume per atom V , $h = 1.5$ cm and $r = 5 \mu\text{m}$, it is found at $T = 83.95$ K, $P_0^* = 525.9$ Torr to be compared with $P_0 = 525.85$ Torr. It should be noted that it is the surface tension term that contributes primarily to the correction, of about 10^{-4} .

Figure 3 shows the fit to the form $\Delta m/m = (B \log P_0^*/P)^x$ of the data obtained with P100 and P120 fibers along the isotherms $T = 83.95$ K and $T = 83.78$ K, respectively. The best fits are obtained with $P_0^* = 526.04$ Torr and $P_0^* = 519.28$ Torr and $x = -0.31 \pm 0.01$.

Below the triple-point temperature we used our data to check the relation

$$d = \left(A \frac{T_3 - T}{T_3} \right)^x,$$

where d is the film thickness at saturation and

$$A = \frac{K_B T T_3}{\alpha} \left(\frac{\partial \ln P_0}{\partial T}_{\text{solid}} - \frac{\partial \ln P_0}{\partial T}_{\text{liquid}} \right).$$

This relation has been derived [18, 19] assuming a *liquid* interface between the solid film and the vapor, with $(T_3 - T)/T_3 \ll 1$. Therefore, we plotted the adsorbed mass at P_0 as $\log(\Delta m/m)$ vs. $\log \{(T/T_3)((T_3 - T)/T_3)\}$.

The straight lines in fig. 4 are the result of the fit, with T_3 as free parameter, for two sets of measurements taken with P100 and P120 fibers, respectively. The temperature T_3 and

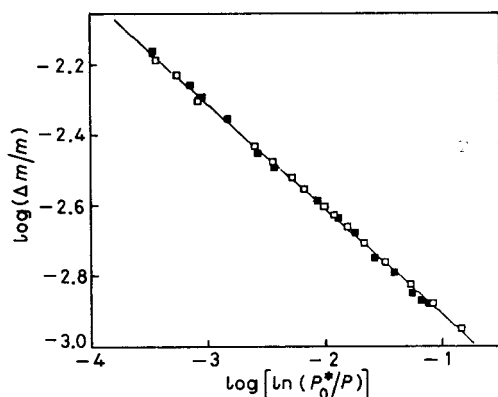


Fig. 3.

Fig. 3. – The fractional mass change $\Delta m/m$ due to gas adsorption along two isotherms above T_3 with P100, $T = 83.95$ K, $P_0^* = 526.04$ Torr (■) and P120, $T = 83.84$ K, $P_0^* = 519.28$ Torr (□), fibers. $\Delta m/m$ is calculated by subtracting the hydrodynamic shift from the measured resonant frequency. P_0^* is the «corrected vapor pressure» calculated as explained in the text.

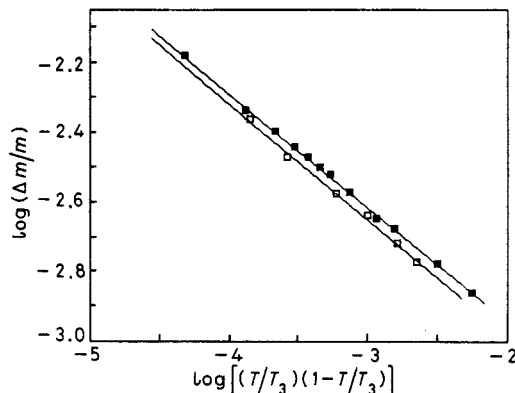


Fig. 4.

Fig. 4. – $\Delta m/m$ for ■: P100 ($x = -0.327$) and □: P120 ($x = -0.333$) fibers along the solid-vapor coexistence curve. $T = 83.77$ K.

the exponent x are found to be (83.77 ± 0.03) K and -0.33 ± 0.01 , for both fibers. Our result for x is in excellent agreement with the $-1/3$ value expected for a van der Waals system [18]. The divergence at T_3 is a consequence of a wetting transition [18, 19].

Our result of noncomplete wetting below T_3 contradicts the conclusion suggested by RHEED experiments. This disagreement may be due either to an incorrect extrapolation of low-temperature behavior up to the region close to T_3 , or to a different surface quality of our substrate with respect to the graphite used in RHEED experiments.

The surface cleanliness of our fibers is expected to be very good owing to the substrate heating prior to performing gas adsorption, as noted by several authors [20]. X-ray line broadening studies performed at Amoco [21], on the other hand, yield length exceeding 200 Å for the size of single domain crystallites in P100 and P120 fibers, thus suggesting a good surface homogeneity. The surface homogeneity and cleanliness of our P120 fiber, however, has been independently checked by us by measuring the mass loading at low-temperature. In fig. 5 a typical run performed at $T = 83.84$ K shows clearly two steps due to the second- and third-layer formation. Our results obtained at four different temperatures are summarized in the insert of fig. 5, and they exhibit a very good agreement with the results obtained by other authors with exfoliated graphite [22, 23]. This leads us to conclude that the adsorption surface in our fibers is primarily that of the basal plane and the surface homogeneity and crystallite size is not significantly different from that of exfoliated graphite substrate.

In conclusion: our result shows that the growth mode of Ar on graphite is characterized by a wetting transition at the bulk triple temperature T_3 , similar to a large number of adsorption systems [2, 3, 10, 19], where wetting is incomplete below T_3 and complete above. It also indicates that it is not valid to infer complete wetting growth behavior based on layer by layer formation for the first several layers [5]. We found the growth mode above T_3 to be in complete agreement with the Frenkel-Halsey-Hill theory [24]. The $1/3$ power law is generally expected to be valid up to 30 layers: beyond that thickness the retardation effect should become important. Recent calculations [25], however, suggest that finite size-boundary effects actually overwhelm the retardation effect.

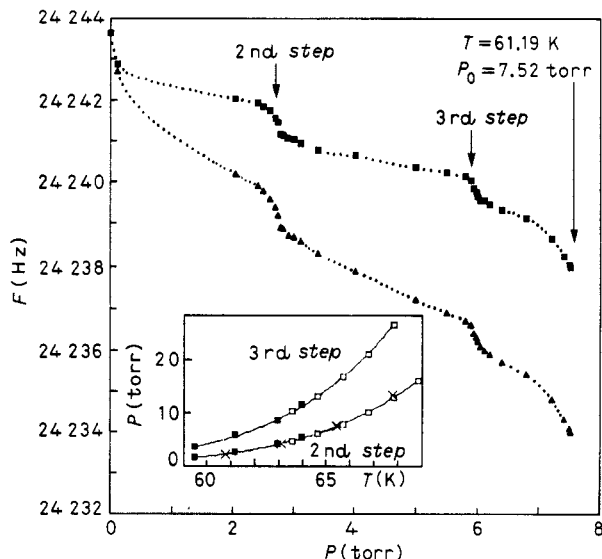


Fig. 5. – The resonant frequency measured along an isotherm with a P120 fiber (full triangles). The full squares indicate the frequency corrected for hydrodynamic shift. The dotted lines are simply eye guides. The insert shows the pressure values corresponding to the 2nd and 3rd layer completion at various temperatures. Crosses and full lines: ref. [22], open squares: ref. [23], full squares: this work $F(\text{cor})$, $F(\text{meas})$ \blacktriangle . The relative frequency shift corresponding to one absorbed layer is $\Delta F/F = 2 \cdot 10^{-5}$; $T = 61.19$ K, $P_0 = 7.52$ Torr.

The growth of Kr and Xe on graphite is presently being investigated to ascertain the theoretical expectation for nonwetting growth due to structural mismatch of solid films [4] to be a universal phenomenon.

* * *

The present work is supported by Consiglio Nazionale delle Ricerche, and in part by NATO under Grant No. 780/85. We are also indebted to M. SANTINI, F. BORGHESANI, P. MISTURA, M. COLE and G. ZIMMERLI for fruitful discussions and suggestions. M. W. H. CHAN wishes to thank the John Simon Guggenheim Memorial Foundation for support.

REFERENCES

- [1] PANDIT R., SCHICK M. and WORTIS M., *Phys. Lett. B*, **26** (1982) 5112.
- [2] DIETRICH S., in *Phase Transitions and Critical Phenomena*, Vol. 12, edited by C. DOMB and J. LIEBOWITZ (Academic Press, New York, N.Y.) 1987.
- [3] BIENFAIT M., *Surf. Sci.*, **162** (1985) 411.
- [4] EBNER C., ROTTMAN C. and WORTIS M., *Phys. Rev. B*, **28** (1983) 4126; GITTES F. T. and SCHICK M., *Phys. Rev. B*, **30** (1984) 209; HUSE D. A., *Phys. Rev. B*, **29** (1984) 6985.
- [5] SEGUIN J. L., SUZANNE J., BIENFAIT M., DASH J. G. and VENABLES J. A., *Phys. Rev. Lett.*, **51** (1983) 122; BIENFAIT M., SEGUIN J. L., SUZANNE J., LERNER E., KRIM J. and DASH J. G., *Phys. Rev. B*, **29** (1984) 983.
- [6] TOUGH J. T., MCCORMICK W. D. and DASH J. G., *Phys. Rev.*, **132** (1963) 2373.
- [7] BRUSCHI L. and SANTINI M., *Rev. Sci. Instrum.*, **46** (1975) 1560.
- [8] BRUSCHI L., MAZZI G., SANTINI M. and TORZO G., *J. Low Temp. Phys.*, **18** (1975) 487; **29** (1977) 63.

- [9] BRUSCHI L. and SANTINI M., *Phys. Lett. A*, **73** (1979) 395; BRUSCHI L., *Nuovo Cimento D*, **1** (1982) 361.
- [10] BARTOSCH C. E. and GREGORY S., *Phys. Rev. Lett.*, **54** (1985) 2513.
- [11] TABOREK P. and SENATOR L., *Phys. Rev. Lett.*, **57** (1986) 218.
- [12] BRUSCHI L. and TORZO G., *Rev. Sci. Instrum.*, **58** (1987) 2181; BRUSCHI L., STORTI R. and TORZO G., *Rev. Sci. Instrum.*, **58** (1987) 1960.
- [13] BRUSCHI L., STORTI R. and TORZO G., *Rev. Sci. Instrum.*, **57** (1986) 2361.
- [14] STOKES G. G., *Mathematical and Physical Papers*, Vol. 3 (Cambridge University Press, London) 1901, p. 38.
- [15] ZIEGLER W. T., MULLINS J. C. and KIRK B. S., Tech. Report No. 2, Project A-460, Georgia Institute of Technology (1962), and FLUBACHER P., LEADBETTER A. J. and MORRISON J. A., *Proc. Phys. Soc. London*, **78** (1961) 1449.
- [16] MIGONE A., DASH J. G., SCHICK M. and VILCHES O., *Phys. Rev. B*, **34** (1986) 6322.
- [17] TABOREK P., unpublished.
- [18] HAUGE E. H., *Fundamental Problems in Statistical Mechanics*, Vol. 6, edited by E. D. G. COHEN (Elsevier, Houston, Tex.) 1985.
- [19] KRIM J., DASH J. G. and SUZANNE J., *Phys. Rev. Lett.*, **52** (1984) 640.
- [20] KRAMER H. M., *J. Cryst. Growth*, **33** (1976) 65; PRICE G. L. and VENABLES J. A., *Surf. Sci.*, **49** (1975) 264.
- [21] BACON R., Amoco Performance Product Inc., private communication.
- [22] GILQUIN B., Note CEA-N-2091 (1979).
- [23] DEMETRIO DE SOUZA J. L. M. and LERNER E., *J. Low. Temp. Phys.*, **66** (1987).
- [24] FRENKEL J., *Kinetic Theory of Liquid* (Oxford, N.Y.) 1949; HALSEY jr. G. D., *J. Chem. Phys.*, **16** (1948) 931; HILL T. L., *J. Chem. Phys.*, **17** (1949) 590.
- [25] MAHALE N. K. and COLE M. W., *Surf. Sci.*, **172** (1986) 311.